Metastable vortex states in $YBa_2Cu_3O_{7-\delta}$ crystal

Y. Radzyner
Department of Physics, Institute of Superconductivity, Bar-Ilan University, 52900 Ramat-Gan, Israel

S. B. Roy
Department of Physics, Institute of Superconductivity, Bar-Ilan University, 52900 Ramat-Gan, Israel and Low Temperature Physics Group, Centre for Advanced Technology, 452013 Indore, India

D. Giller
Department of Physics, Institute of Superconductivity, Bar-Ilan University, 52900 Ramat-Gan, Israel

Y. Wolfus
Department of Physics, Institute of Superconductivity, Bar-Ilan University, 52900 Ramat-Gan, Israel

A. Shaulov
Department of Physics, Institute of Superconductivity, Bar-Ilan University, 52900 Ramat-Gan, Israel

P. Chaddah
Low Temperature Physics Group, Centre for Advanced Technology, 452013 Indore, India

Y. Yeshurun
Department of Physics, Institute of Superconductivity, Bar-Ilan University, 52900 Ramat-Gan, Israel

(Received 10 January 2000)

Magnetization measurements in an untwinned $YBa_2Cu_3O_{7-\delta}$ crystal reveal a range of temperatures and fields for which the magnetization exhibits unusual history-dependent behavior. This range envelopes the transition line, $B_{ss}(T)$, separating between the vortex quasiordered and disordered phases. The observed history effects indicate that a disordered (quasiordered) vortex state can exist as a metastable state below (above) the $B_{ss}(T)$ line. The fields, defining the phase transition and the borders of the metastability region, are correlated to sharp features in the magnetization loop.

The field-temperature (B-T) phase diagram of the vortex matter in superconductors is a subject of extensive research. Recent experimental[1–8] and theoretical[9–13] studies have indicated the existence of two distinct vortex solid phases: A quasiordered phase (Bragg glass) at low fields and a highly disordered, entangled, phase (vortex glass) at high fields. A transition between these two vortex solid phases, associated with the second magnetization peak (''fishtail''), has been observed in $Bi_2Sr_2CaCu_2O_{8+\delta}$ (BSCCO),[4] $Nd_{1.85}Ce_{0.15}CuO_{4-\delta}$,[6] untwinned $YBa_2Cu_3O_{7-\delta}$ (YBCO),[7,8,14] and low-T_c superconductors such as $CeRu_2$ (Ref. 15) and 2H-$NbSe_2$.[16] The relatively broad second peak, measured in untwinned YBCO, exhibits a sharp onset at $B_{\rm onset}$ and a sharp change of slope at $B_{\rm kink}$.[8,17] These two features occur at different fields on the ascending and descending branches of the magnetization loop, resulting in four different characteristic fields: $B^+_{\rm onset}, B^-_{\rm onset}, B^+_{\rm kink}$, and $B^-_{\rm kink}$. The significance of these four fields has not yet been clarified. In this paper we correlate these characteristic fields to the vortex solid-solid transition field, B_{ss}, and to the limits of metastability of the vortex state on ascending and descending fields.

The existence of metastable vortex states, in the region of the fishtail, was reported for low-T_c materials, such as $CeRu_2$,[18] 2H-$NbSe_2$,[16,19] Nb,[20] and Nb_3Ge films.[21] Direct observation of metastable vortex states, utilizing magneto-optical imaging techniques, has recently been reported for BSCCO.[22] Similar magneto-optical measurements in YBCO are impossible at present, because of the relatively large transition field (order of Tesla, well above the saturation field of iron-garnet indicators[23]). By employing a Hall array for local magnetization measurements we demonstrate the existence of metastable vortex states in YBCO, and identify the limits of the region of metastability. This is achieved by comparing magnetization curves, measured after various cooling or heating protocols, with the ''complete'' loop (isothermal M-H envelope curve) measured after a conventional zero-field-cooling process. We identify a strip in the field-temperature phase diagram, for which—contrary to the expectations from the Bean model[24]—the magnetization is history dependent even after several, relatively large, field steps. This strip, bounded by $B^-_{\rm onset}$ from below and by $B^+_{\rm kink}$ from above, is identified as a vortex metastability region.

The $0.5\times0.3\times0.02$ mm^3 untwinned YBCO crystal[25] ($T_c\cong93$ K) used in Ref. 8, was in direct contact with an array of 10×10 μm^2 Hall sensors (sensitivity better than 0.1 G). The results reported in this paper utilize two sensors, one close to the sample's center and another just outside the sample.

The inset to Fig. 1 exhibits a typical hysteresis loop, measured at $T=55$ K after zero-field cooling the sample from

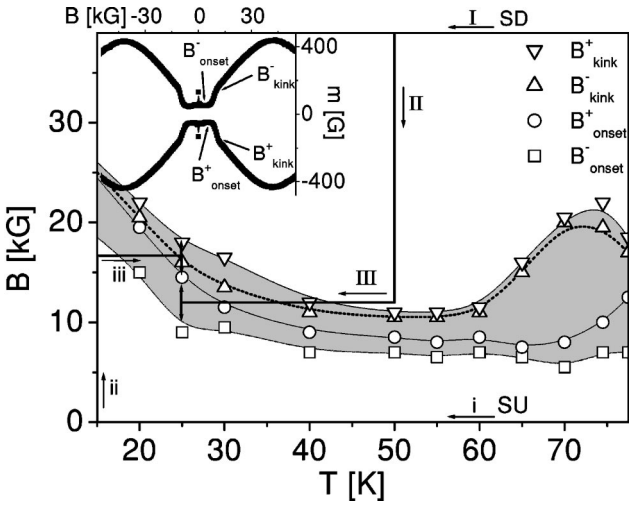

FIG. 1. Magnetic phase diagram for the $YBa_2Cu_3O_{7-\delta}$ crystal showing four lines: $B^-_{\rm onset}$ (squares), $B^+_{\rm kink}$(down triangles), $B^-_{\rm kink}$ (up triangles), $B^+_{\rm onset}$ (circles), lines are guides to eye. The shaded area between $B^-_{\rm onset}$ and $B^+_{\rm kink}$ is identified as the region of metastability. Arrows with capital roman numerals track step-down (SD) procedure. Arrows and small roman numerals follow step-up (SU) procedure. Inset: magnetization loop at $T=55$ K, with arrows pointing to relevant features.

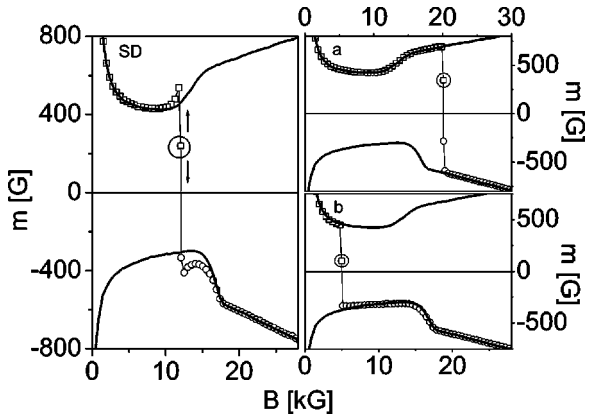

FIG. 2. Left: Complete loop at 25 K (solid line) and magnetization data following SD procedure with $H_{\rm target}=12$ kOe: Decreasing field (open squares) and increasing field (open circles). Right: Same measurement with $H_{\rm target}=20$ kOe (a) and $H_{\rm target}=5$ kOe (b). Starting point is encircled, arrows point in direction of change in field.

above T_c. The external magnetic field is varied from -60 to 60 kOe in steps of 500 Oe. The four characteristic fields: $B^+_{\rm onset}$, $B^-_{\rm onset}$, $B^+_{\rm kink}$, and $B^-_{\rm kink}$ are marked by arrows. The temperature dependence of these fields is plotted in Fig. 1. The nonmonotonic behavior of these curves is consistent with previous reports for untwinned YBCO.[8,14,17]. Note that $B^+_{\rm onset}$ and $B^+_{\rm kink}$ are larger than $B^-_{\rm onset}$ and $B^-_{\rm kink}$, respectively. The shaded area between the two extreme lines, $B^-_{\rm onset}$ and $B^+_{\rm kink}$, plays a major role in the discussion below. For the purpose of clarity, all other lines in the phase diagram (irreversibility line, melting line, etc.) are eliminated from the figure; See Ref. 8 for the full phase diagram. In contrast with the phase diagram of NCCO (Ref. 6) and BSCCO,[4] the solid-solid transition region in YBCO is flat around 50 K and ascends towards both high temperatures[7,8,14,17] and low temperatures. The increase toward high temperature, may be attributed to the weakening of the pinning energy, resulting from the increase of thermal fluctuations, which occurs when the depinning temperature is crossed.[8] An increase towards low temperatures was observed in NCCO,[28] and was attributed to Bean-Livingston barriers.

At this point of our discussion it is not yet clear which one of the four characteristic fields plotted in Fig. 1 marks the vortex solid-solid transition line. However, it is clear that below the shaded area the vortex phase is quasiordered, and above this area the vortex phase is disordered. The purpose of the experiments described below is to identify the vortex state in the shaded area of Fig. 1.

The first experiment presented follows a ''step-down'' (SD) field-cooling protocol, depicted by a solid line and capital numerals in Fig. 1. The experiment consists of the following steps: (I) The sample is cooled from above T_c to 50 K in the presence of an external field of 40 kOe. (II) At 50 K the field is lowered to $H_{\rm target}=12$ kOe in steps of 500 Oe. (III) At $H=H_{\rm target}$ the temperature is lowered to 25 K. This point, which is located within the shaded area, is the starting point for the magnetization measurements. The purpose of the previous three steps is to emulate a field cooling process while circumventing the high-temperature peak of the shaded area. At 25 K the magnetization is measured while the field is either decreased to 0 or increased to 60 kOe, in steps of 500 Oe.

The results of this experiment are presented on the left-hand side of Fig. 2. Evidently, the measured magnetization exhibits a significant *overshoot* compared to the complete loop, in both descending (open squares) and ascending (open circles) branches. Note that on the ascending branch the measured magnetization merges with the complete loop at $B^+_{\rm kink}$, while on the descending branch this convergence occurs around $B^-_{\rm onset}$.

We repeated the same SD procedure with $H_{\rm target}=5$ and 20 kOe, producing starting points of the measurements below and above the shaded area, respectively. The results, presented on the right-hand side of Fig. 2, show overlap of the measured magnetization with the complete hysteresis loop after the field is changed by $2H^*$ at most, as expected from the Bean model.[24] (The depth of the induction profile H^* is in the range of 500 Oe in our experiment).

In a second set of experiments, referred to as ''step-up'' (SU) protocol, we arrive at the starting point of the magnetization measurement by a different route, depicted in Fig. 1 by solid lines and small numerals. This procedure consists of the following steps: (i) The sample is cooled in zero field to 15 K. (ii) At 15 K the field is raised to $H_{\rm target}=16.5$ kOe in steps of 500 Oe. (iii) The temperature is then raised to 25 K at $H=H_{\rm target}$. This is the starting point of the measurement, which is again located within the shaded area. At 25 K the magnetization is measured while the field is increased to 30 kOe, in steps of 500 Oe.

The results of this experiment are presented on the left-hand side of Fig. 3 (solid circles). In this case, the measured magnetization exhibits an *undershoot* compared to the complete loop. Note that the magnetization curve merges with the ascending branch of the complete loop at $B^+_{\rm kink}$, as in the previous case.

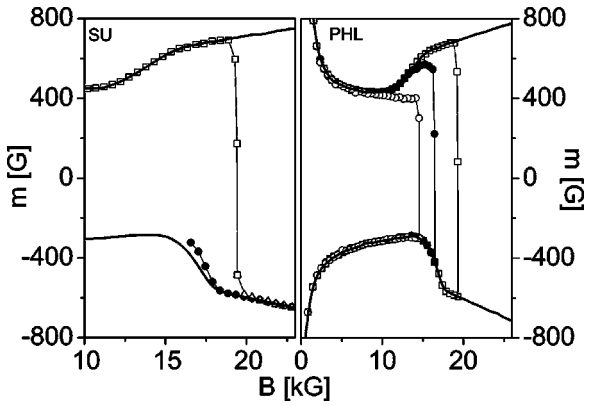

FIG. 3. Left: Complete loop at 25 K (solid line) and magnetization data following SU procedure with $H_{\text{target}}=16.5$ kOe (solid circles), $H_{\text{target}}=20$ kOe (open squares for descending fields, open triangles for increasing field). Right: Partial hysteresis loops (PHL) at 25 K, corresponding to a maximum field of 16.5 kOe (solid circles), 15 kOe (open circles), and 19.5 kOe (open squares).

We repeated the same SU procedure with $H_{\text{target}}=20$ kOe, producing a starting point of the measurements above the shaded area. The results, presented on the left-hand side of Fig. 3 (open squares for descending field, open triangles for ascending field), show overlap of the measured magnetization with the complete hysteresis loop after the field is changed by $2H^*$ at most.[24]

The third set of experiments is that of partial (or ''minor'') hysteresis loops.[15,26] In these experiments the ascent of the field is terminated at a field smaller than the maximum field of the complete loop. Figure 3 (right-hand side) describes results of partial loop measurements at 25 K with maximum fields of 15 kOe (open circles) and 16.5 kOe (solid circles). In both measurements, the point where the field begins its descent is again located within the shaded area. The results show an overlap of the ascending branches, as expected. However, a significant undershoot of the descending branches of the partial loops, as compared to the complete loop, is observed. Note that, as in the first experiment (Fig. 2), the descending branches of the partial loops merge with the descending branch of the complete loop around B^-_{onset}. This observation is consistent with that reported in Ref. 26.

The partial loop experiment was repeated with maximum field of 20 kOe (Fig. 3, right). In this measurement the field begins its descent at a point located *above* the shaded area of the phase diagram. The results show overlap of the descending branch of the measured partial loop with the complete hysteresis loop after the field is changed by $2H^*$ at most.[24]

All experiments described above indicate that the starting point of the measurement plays a critical role. In the first and second sets of experiments the starting point, where the magnetization measurements begin, is the end point of the SU and SD protocols. In the partial loop measurements the starting point is the point where the field begins its descent. The results of all these experiments can be summarized as follows: (a) If the starting point of the measurement is inside the shaded area of Fig. 1, the measured magnetization does not overlap with the complete loop, despite having changed the field by more than $2H^*$. (b) The magnetization overshoots the complete loop if the starting point is reached via the disordered state (i.e., from above the shaded area). It undershoots, if the starting point is arrived at from the quasiordered state (below the shaded area). (c) In all experiments, regardless of the history of the travel to the starting point, the curves merge with the complete loop at B^+_{kink} for ascending fields and at B^-_{onset} for descending fields. (d) If the starting point of the measurement is outside the metastability region, the magnetization overlaps with the complete loop, within the mandatory $2H^*$.[24] It is clear that history dependence is not an inherent property of either phase but of the phase transition itself, in contrast to Ref. 26.

In the following we argue that the above results indicate that in the shaded area of the B-T phase diagram (Fig. 1), disordered or quasiordered states can exist as metastable states. In the first experiment, while cooling the sample from 50 to 25 K, we actually ''freeze'' the disordered phase at 50 K and ''drag'' (or ''supercool'') it into the region where it can exist as a metastable state. This is manifested by the overshoot of the SD curves (Fig. 2), signifying a higher persistent current that characterizes the disordered phase. The inductions B^+_{kink} and B^-_{onset}, where the SD curve and the complete loop merge, indicate the limits of the metastability zone.

One can explain the results of the second set of experiments in a similar manner. While heating the sample from 15 to 25 K at a constant field of 16.5 kOe, the quasiordered state produced at 15 K is dragged (or superheated) into a region where it can exist as a metastable quasiordered state. This is manifested by the undershoot of the SU curve (Fig. 3, left), signifying a lower persistent current that characterizes the quasiordered phase. As expected, the SU curve merges with the complete loop at the upper limit of the metastability region, namely at B^+_{kink}, as in previous experiments.

The results of the third set of experiments, namely the partial hysteresis loops (Fig. 3, right), are interpreted in a consistent way: the descending branch of the complete loop retains the disorder produced at very high fields, well above B^+_{kink}. The descending branch of the partial loop retains the disorder produced before the field culminates. As is evident from the right-hand side of Fig. 3, the disorder retained by the complete loop is larger than that of the partial loop. Here, again, the partial loop converges with the full loop at B^-_{onset}, which is the lower limit of the metastability region.

On the basis of the above interpretation we conclude that the $B^+_{\text{kink}}(T)$ and $B^-_{\text{onset}}(T)$ lines determine the borders of the region where metastable states may exist. The quasiordered phase may exist as a metastable phase in the range $B_{ss}<H<B^+_{\text{kink}}$. The disordered phase may exist as a metastable phase in the range $B^-_{\text{onset}}<H<B_{ss}$. In the following we explain the significance of the other two lines, which appear in the phase diagram, namely $B^+_{\text{onset}}(T)$ and $B^-_{\text{kink}}(T)$.

Recent experiments in BSCCO (Ref. 22) revealed that an abrupt change in the external field causes the injection of a transient disordered vortex state into the sample. This can be ascribed, for example, to surface imperfections and/or surface barriers, which impede ''smooth'' entrance of the injected fluxons, as demonstrated by Paltiel *et al.* in $NbSe_2$.[27] When the thermodynamic conditions dictate a quasiordered state, the injected transient disordered state relaxes into a quasiordered state at a rate decreasing to zero as the induction approaches B_{ss}. Our procedures involve steps of 500 Oe

between adjacent measurements. Thus, generation of a transient disordered state can be expected after each step. Below B^{+}_{onset} there is no change in the persistent current, implying that the lifetime of this transient state is much smaller than our time window and therefore a quasiordered state is measured. However, as B^{+}_{onset} is approached, the lifetime of the transient disordered state is comparable to the time window of the measurement and therefore a larger persistent current is measured, indicating the existence of a disordered state. Reaching the higher limit for metastability, B^{+}_{kink}, the disordered phase becomes the stable, thermodynamic phase.

The remaining feature, B^{-}_{kink}, cannot be associated with the lifetime of the transient disordered state. This is because above the metastability region the thermodynamics dictate a disordered state, so that the phase introduced by the change of field does not alter the phase already existing in the sample. Thus, it is natural to associate B^{-}_{kink} with the thermodynamic transition field, B_{ss}. After crossing this transition line, vortex matter gradually becomes ordered and the magnetization smaller, until B^{-}_{onset} is crossed and the matter becomes completely ordered.

In conclusion, we have shown the existence of a region in the B-T phase diagram of YBCO, where the vortex matter can persist in a metastable state. The limits of this region are $B^{-}_{\mathrm{onset}}(T)$ and $B^{+}_{\mathrm{kink}}(T)$. The vortex solid-solid transition line is identified as $B^{-}_{\mathrm{kink}}(T)$. The field $B^{+}_{\mathrm{onset}}(T)$ is associated with a transient disordered vortex state generated by a step in the external field. The existence of the metastability region indicates that the vortex solid-solid transition may be a first-order transition.

This research was supported by the Israel Science Foundation founded by the Israel Academy of Sciences and Humanities–Center of Excellence Program, and by the Heinrich Hertz Minerva Center for High Temperature Superconductivity. Y.Y. acknowledges support from the U.S.-Israel Binational Science Foundation. D.G. acknowledges support from the Clore Foundation. S.B.R. acknowledges the warm hospitality at Bar-Ilan.

[1] R. Cubitt, E.M. Forgan, G. Yang, S.L. Lee, D. Paul, H.A. Mook, M. Yethiraj, P.H. Kes, T.W. Li, A.A. Menovsky, Z. Tarnawski, and K. Mortensen, Nature (London) **365**, 407 (1993).

[2] S.L. Lee, P. Zimmermann, H. Keller, M. Warden, R. Schauwecker, D. Zech, R. Cubitt, E.M. Forgan, P.H. Kes, T.W. Li, A.A. Menovsky, and Z. Tarnawski, Phys. Rev. Lett. **71**, 3862 (1993).

[3] E. Zeldov, D. Majer, M. Konczykowski, V.B. Geshkenbein, V.M. Vinokur, and H. Shtrikman, Nature (London) **375**, 373 (1995).

[4] B. Khaykovich, E. Zeldov, D. Majer, T.W. Li, P.H. Kes, and M. Konczykowski, Phys. Rev. Lett. **76**, 2555 (1996).

[5] A. Schilling, R.A. Fisher, N.E. Phillips, U. Welp, W.K. Kwok, and G.W. Crabtree, Phys. Rev. Lett. **78**, 4833 (1997).

[6] D. Giller, A. Shaulov, R. Prozorov, Y. Abulafia, Y. Wolfus, L. Burlachkov, Y. Yeshurun, E. Zeldov, V.M. Vinokur, J.L. Peng, and R.L. Greene, Phys. Rev. Lett. **79**, 2542 (1997).

[7] T. Nishizaki, T. Naito, and N. Kobayashi, Phys. Rev. B **58**, 11 169 (1998).

[8] D. Giller, A. Shaulov, Y. Yeshurun, and J. Giapintzakis, Phys. Rev. B **60**, 106 (1999).

[9] T. Giamarchi and P. Le Doussal, Phys. Rev. Lett. **72**, 1530 (1994).

[10] T. Giamarchi and P. Le Doussal, Phys. Rev. B **52**, 1242 (1995); **55**, 6577 (1997).

[11] V. Vinokur, B. Khaykovich, E. Zeldov, M. Konczykowski, R.A. Doyle, and P.H. Kes, Physica C **295**, 3 (1998).

[12] D. Ertas and D.R. Nelson, Physica C **272**, 1 (1996).

[13] J. Kierfeld, Physica C **300**, 171 (1998).

[14] K. Deligiannis, P.A.J. de Groot, M. Oussena, S. Pinfold, R. Langan, R. Gagnon, and L. Taillefer, Phys. Rev. Lett. **79**, 2121 (1997).

[15] S.B. Roy and P. Chaddah, Physica C **279**, 70 (1997).

[16] G. Ravikumar, V.C. Sahni, P.K. Mishra, T.V. Chandrasekhar Rao, S.S. Banerjee, A.K. Grover, S. Ramakrishnan, S. Bhattacharya, M.J. Higgins, E. Yamamoto, Y. Haga, M. Hedo, Y. Inada, and Y. Onuki, Phys. Rev. B **57**, R11 069 (1998).

[17] T. Nishizaki, T. Naito, S. Okayasu, A. Iwase, and N. Kobayashi, Phys. Rev. B **61**, 3649 (2000).

[18] S.B. Roy, P. Chaddah, and S. Chaudhary, J. Phys.: Condens. Matter **10**, 4885 (1998); **10**, 8327 (1998).

[19] W. Henderson, E.Y. Andrei, M.J. Higgins, and S. Bhattacharya, Phys. Rev. Lett. **77**, 2077 (1996).

[20] M. Steingart, A.G. Putz, and E.J. Kramer, J. Appl. Phys. **44**, 5580 (1973).

[21] R. Wordenweber, P.H. Kes, and C.C. Tsuei, Phys. Rev. B **33**, 3172 (1986).

[22] D. Giller, A. Shaulov, T. Tamegai, and Y. Yeshurun, Phys. Rev. Lett. **84**, 3698 (2000).

[23] V. K. Vlasko-Vlasov, G. W. Crabtree, U. Welp, and V. I. Nikitenko, in *Physics and Materials Science of Vortex States, Flux Pinning and Dynamics*, edited by R. Kossowsky, S. Bose, V. Pan, and Z. Durusoy (Kluwer Academic, Dordrecht, 1999), Vol. 356, p. 205.

[24] C.P. Bean, Phys. Rev. Lett. **8**, 250 (1962).

[25] J.P. Rice and D.M. Ginsberg, J. Cryst. Growth **109**, 1 (1991).

[26] S. Kokkaliaris, P.A.J. de Groot, S.N. Gordeev, A.A. Zhukov, R. Gagnon, and L. Taillefer, Phys. Rev. Lett. **82**, 5116 (1999).

[27] Y. Paltiel, E. Zeldov, Y.N. Myasoedov, H. Shtrikman, S. Bhattacharia, M.J. Higgins, Z.L. Xiao, E.Y. Andrei, P.L. Gammel, and D.J. Bishop, Nature (London) **403**, 398 (2000).

[28] M.C. de Andrade, N.R. Dilley, F. Ruess, and M.B. Maple, Phys. Rev. B **57**, R708 (1998).